Hindawi
Geofluids
Volume 2022, Article ID 6220549, 15 pages
https://doi.org/10.1155/2022/6220549

Research Article

Mechanical Behavior of Cracked Rock in Cold Region Subjected to Step Cyclic Loading

Liang Zhang,[1,2] **Fujun Niu**,[1] **Minghao Liu**,[1] **Jing Luo**,[1] **and Xin Ju**[1,2]

[1]*State Key Laboratory of Frozen Soil Engineering, Northwest Institute of Eco-Environment and Resources, Chinese Academy of Sciences, Lanzhou 730000, China*
[2]*University of Chinese Academy of Sciences, Beijing 100049, China*

Correspondence should be addressed to Fujun Niu; niufujun@lzb.ac.cn and Minghao Liu; liuminghao@lzb.ac.cn

Received 15 November 2021; Revised 24 December 2021; Accepted 27 December 2021; Published 17 January 2022

Academic Editor: Dongdong Ma

In order to analyze the mechanical behavior of cracked rock in cold region subjected to cyclic loading, step cyclic loading and unloading (SCLU) triaxial tests with different stress paths have been designed. The mechanical responses such as strength, deformation, and failure mode were analyzed. The test results show that limestone has obvious strengthening effect under cyclic loading due to local crushing and filling of internal structural plane. The strengthening effect and fatigue damage effect caused by cyclic loading and the impact damage effect caused by the upgraded of stress level have an effect on mechanical response of cracked rock, and the degree of influence is related to the stress path. Under the stress path of constant stress lower limit (CSLL), the strengthening effect of rock was more prominent and its strength was enhanced. It was mainly subjected to progressive fatigue damage and had a buffering effect in the failure process. However, under the stress path of increasing the stress lower limit (ISLL), the rock suffered significant impact damage and entered the fatigue damage stage in advance, which led to its strength reduction and sudden failure when entering the next stress level. In addition, during the loading process, larger initial stress amplitudes led to more obvious cyclic strengthening effects, while smaller initial stress amplitudes led to greater plastic deformation and energy dissipation, and the rock was more prone to progressive damage.

1. Introduction

Traditional studies on rock mechanical behavior mostly focus on monotonic loading conditions, while engineering practices show that rock is affected by step cyclic loading and unloading (SCLU) disturbance to varying degrees in the excavation process of high slope, mine roadway, traffic, and hydraulic tunnel, as well as in the operation process of dam storage and flood discharge [1, 2]. With the development of engineering construction in cold regions, the mechanical behavior of cracked rock subjected to step cyclic loading has become a research hotspot of scholars [3–5]. Due to the damage freeze-thaw alternation, rocks in cold regions generally generate cracks [6]. Compaction, development, expansion, convergence, and cracking of irregular interlayer such as primary fissures and joints before rock are completely destroyed, and the most significant manifestation of these evolutionary processes is the change of rock mechanics parameters and energy [7]. Therefore, it is of great significance to study the mechanical parameters and energy evolution law of rock with irregular interlayer under SCLU conditions, which is also helpful to better explain the damage mechanism of rock in practical engineering.

Previous studies on the mechanical properties of rock under cyclic loading and unloading are mainly divided into two aspects. One is to analyze the deformation and strength evolution properties of rock under fatigue damage from macroscopic and microscopic perspectives. The experimental study found that the development of rock deformation during uniaxial cyclic loading compression can be divided into initial stage, stable stage, and acceleration stage [8]. Hu et al. analyzed the stress-strain relationship of granite under different maximum loads, loading amplitude, and loading frequency during cyclic loading and unloading and also found that the cumulative damage presented an obvious three-stage process [5]. Ghamgosar and Erarslan studied the

development and closure of microcracks in the fracture process of tuff under mono-loading and cyclic loading through splitting test and numerical simulation [9]. It was found that cyclic loading caused continuous friction between grains and produced more microcracks, while mono-loading produced a smooth shear band. Ghamgosar et al. also found that cyclic loading would reduce the rock strength to 70% of its original strength, and the high-density microcracks formed were mostly located in the fracture process zone [10]. The second is to establish various damage models combined with the law of energy evolution. The damage process of rock is a kind of energy dissipation process, and the strength, deformation, and failure characteristics of rock have internal relations with energy dissipation [11]. Peng et al. found that the damage model established according to energy evolution is more consistent with the actual damage evolution process of rock [12]. Therefore, many scholars gradually studied the evolution of rock deformation and damage under cyclic loading from the perspective of energy. The variation characteristics of hysteretic cycle curves of typical cyclic loading were analyzed in detail, and the variation rules of parameters such as total work, elastic deformation energy, dissipated energy, energy dissipation rate, residual strain, damage variables, and their mutual relations in the loading and unloading process were discussed [13].

The above studies attempted to reveal the damage evolution law of rock under cyclic loading and unloading from different aspects and obtained valuable results. However, for rock with irregular interlayers, the cyclic loading process not only exist damage evolution but may also exist obvious strengthening effect, resulting in the increase of rock strength [14]. Therefore, it has some limitations to study the mechanical response of irregular interbedded rock materials only from the perspective of damage evolution law. In addition, the research on the mechanical response of rock under cyclic loading mainly focuses on the damage evolution law under constant stress amplitude, while the research on the mechanical response of rock under step cyclic loading of different stress paths is not deep and clear enough. In practical engineering, with the increase of working depth or the change of construction location, the cyclic load stress amplitude and stress lower limit of rock will change differently [15], and therefore, a further study to explore the influence of different stress paths on rock bearing capacity, deformation, and energy dissipation is necessary.

In order to resolve those problems, this article intends to design triaxial SCLU tests with four different stress paths (constant or increasing stress lower limit, relatively large, or small initial stress amplitude), and the corresponding strength, performance parameters, deformation, and energy were calculated according to the stress-strain curves of the rocks. Combined with the structural characteristics of rock with irregular interlayer, the experimental phenomena are analyzed. The study in this paper is helpful to reveal the failure mechanism of rock damage, deterioration, and instability under different SCLU stress paths. The research results of this article have important significance for the design and construction of cracked rock in engineering construction and the prevention and control of dynamic disasters.

2. Rock Specimen Preparation and Test Methods

2.1. Specimen Preparation. As shown in Figure 1, the limestone was chosen from the Nangqian County of Qinghai Province, and CT scan showed that many irregular interlayers existed within it. The proposed tunnel project in this area needs to excavate the rock mass, which may be affected by SCLU during the construction process. The research results of this article will also provide reference for the engineering construction in this area.

The rock blocks were wrapped in foam cotton and transported to the State Key Laboratory of Frozen Soil Engineering, Chinese Academy of Sciences. As shown in Figure 1(c), in strict accordance with the International Society for Rock Mechanics code, the rock block was prepared into a standard cylinder rock sample with a size of φ 50 mm × L100 mm. In order to minimize the influence of heterogeneity of the specimens on the test results, all specimens are drilled from the same rock. Five groups of specimens, #1, #2, #3, #4, and #5, were used in the test. Two additional rock specimens are set in each group for repeated test to reduce the occasionality and error of the experiment.

2.2. Test Equipment. The equipment used was the GCTS RTR-1000 rock triaxial test system of the State Key Laboratory of Frozen Soil Engineering of the Chinese Academy of Sciences. The equipment can perform strain or stress control, as well as conduct behavior tests after rock failure. The maximum axial load of the test equipment is 1000 kN, and the loading frame stiffness is 1750 kN/mm. The integrated confining pressure can reach 140 MPa, the pressure resolution is 0.01 MPa, and the liquid volume resolution is 0.01 CC. The rock specimen size was up to 75 mm (3 inches). The equipment has an axial and radial linear variable differential transformer measurement, deformation range ± 2.5 mm, and deformation resolution of 0.001 mm. The installation of test equipment and rock specimen is shown in Figure 2.

2.3. Test Methods. During the construction of rock excavation, the rock may be affected by SCLU. The cyclic loading form of rock caused by construction activities is related to the change of upper and lower limit of stress and stress amplitude with stress level (for example, when mineral resources enter deep mining, the surrounding rock of the roadway and stope is under different unloading and loading disturbances due to different mining methods, and the failure mode and energy dissipation of the surrounding rock are significantly different.) [16], it is transformed into indoor test settings, corresponding to different stress paths of SCLU. Five different stress paths were designed in this experiment. The corresponding curves of stress and time under different stress paths are shown in Figure 3. In order to reduce the influence of the non-uniformity of samples on the test results, the larger discrete type was removed. The test results were valid only when three or more similar results were obtained.

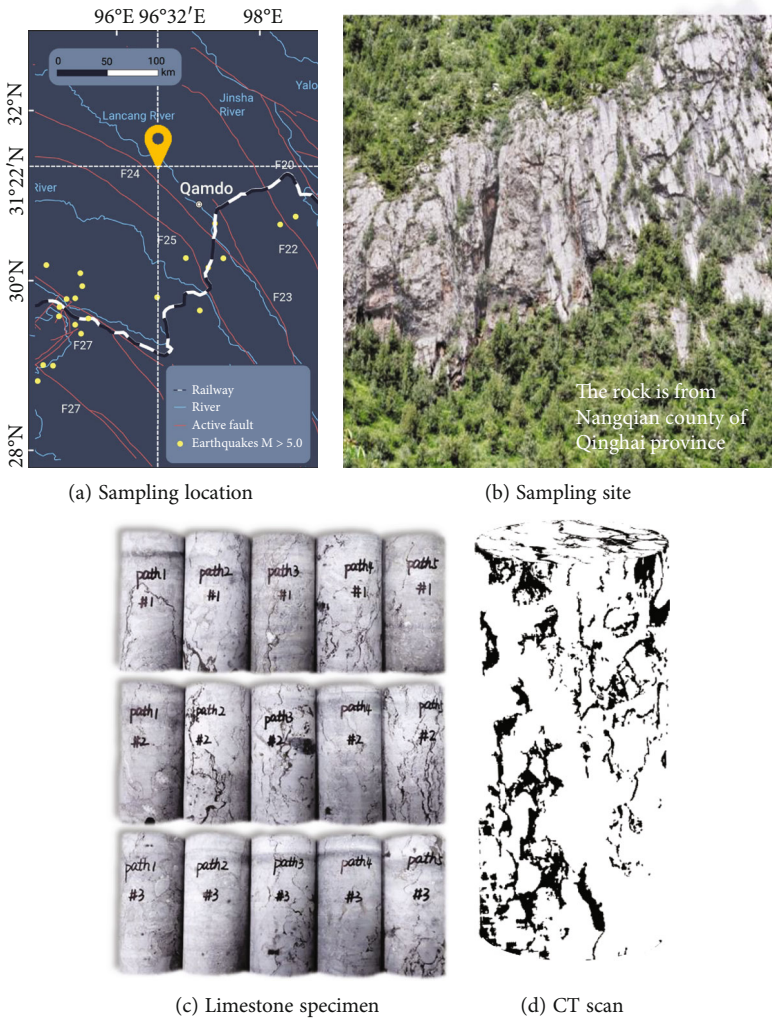

(a) Sampling location (b) Sampling site

(c) Limestone specimen (d) CT scan

Figure 1: Sampling site and specimens.

Figure 2: Test devices.

As shown in Figure 3(a), the stress path 1 is the conventional triaxial compression experiment, and the loading rate is 0.02 mm/min. Stress path 2-5 is triaxial SCLU experiment, which is loaded by axial stress control. The loading waveform is sine wave, frequency is 0.1 Hz, each level has 30 cycles, the period of each cycle is 10s, and the initial value of deviator stress is 1 MPa (which can make the loading device fully contact with the specimen). The loading

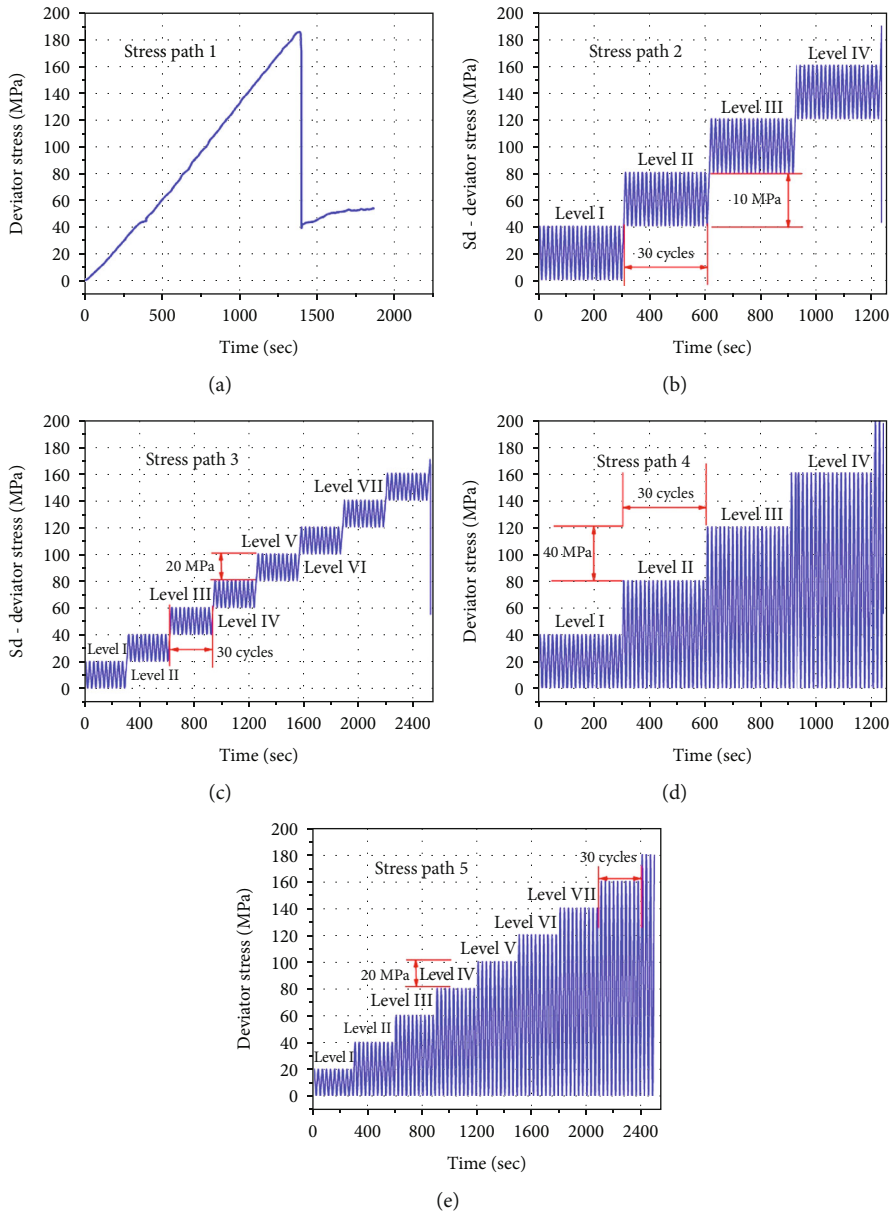

Figure 3: Loading diagram of different stress paths.

Table 1: Loading parameters of each stress path.

Stress path	Increment of upper stress limit at adjacent stress level (MPa)	Increment of lower stress limit at adjacent stress level (MPa)	Initial stress amplitude (MPa)	Stress amplitude at adjacent stress level (MPa)
2	40	40	40	0
3	20	20	20	0
4	40	0	40	40
5	20	0	20	20

parameters of each stress path are shown in Table 1. In the stress path 2, the upper and lower stress limits are both increased by 40 MPa at each stress level, and the stress amplitude is 40 MPa, which remains unchanged. In stress path 3, the upper and lower stress limits are both increased by 20 MPa at each stress level, and the stress amplitude is 20 MPa and remains unchanged. In stress path 4, the lower stress limit is 1 MPa and remains unchanged, and the stress amplitude is improved by 40 MPa at each level of loading. In stress path 5, the lower stress limit is 1 MPa and remains

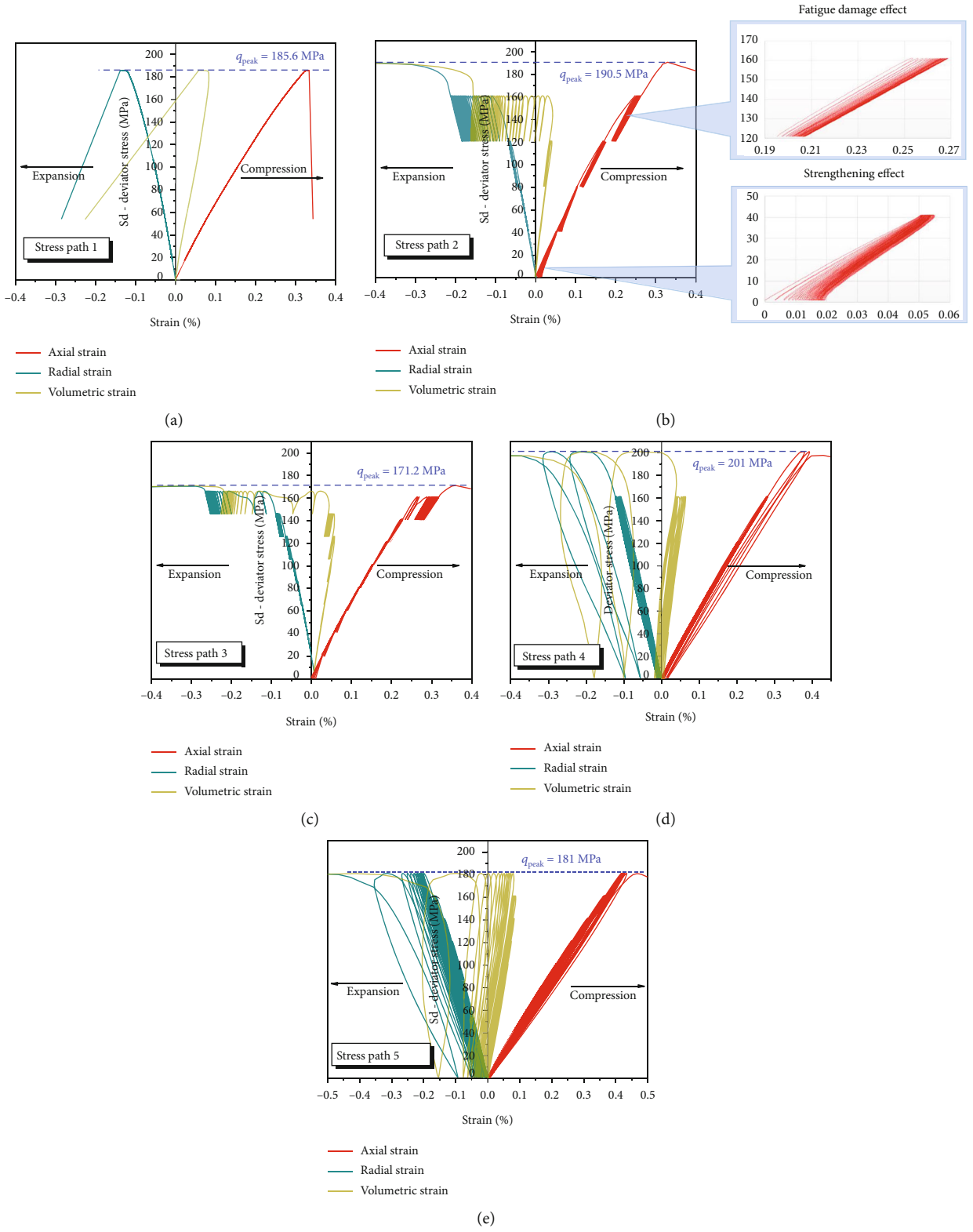

Figure 4: Stress-strain curves of limestone subjected to step cyclic loading.

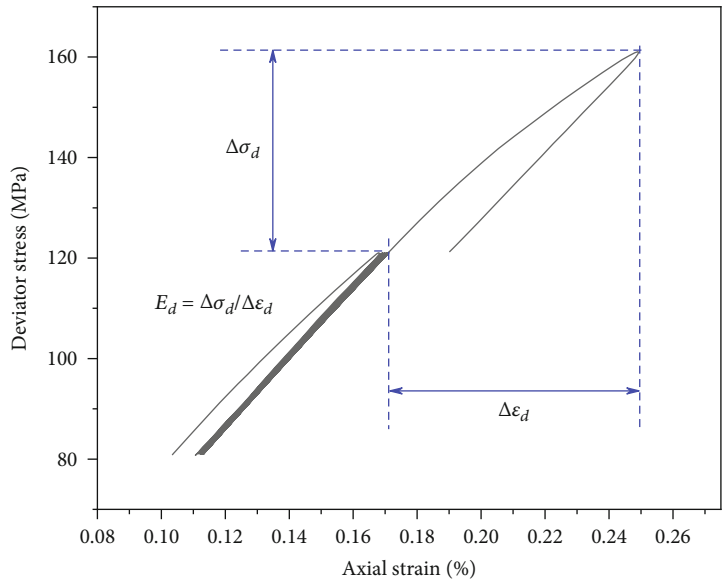

Figure 5: Calculation diagram of dynamic elastic modulus.

unchanged, and the stress amplitude is improved by 20 MPa at each level of loading. In this article, the triaxial loading tests of all stress paths are carried out under the confining pressure of 5 MPa.

3. Test Results and Analysis

3.1. Characteristics of Whole Process Stress-Strain Curves under Step Cyclic Loading Stress Paths. The stress-strain curves of limestone specimens under different stress paths of SCLU are shown in Figure 4. It can be seen from Figure 4(a) that under the condition of conventional triaxial compression (stress path 1), the limestone shows the deformation characteristics of approximate linear relationship until sudden failure occurs, and it is mainly elastic deformation with elastic-brittle properties.

The strength of rock is related to the stress path. It is generally believed that irreversible structural damage will occur in the process of SCLU, and the strength of rock decreases gradually, which is called fatigue damage. However, both seismic observations [17, 18] and laboratory tests [19, 20] can confirm that after structural damage or irreversible deformation of rocks, the strength of rock will increase or recover. This is called cyclic strengthening effect. The reason for this phenomenon is that the improvement of the contact state between the particles increases the friction and contributes to the improvement of the bearing capacity of the rock.

The fatigue damage and strengthening effect are coupled in the process of cycle loading. Taking stress path 2 as an example, as shown in Figure 4(b), at the early stress level of loading, the plastic strain increment after unloading was significantly higher than the peak strain increment under the same stress level, which indicates that the plastic strain increment is mainly caused by the improvement of the contact state between particles under cyclic loading and the strengthening effect is more significant. However, at the later stress level of loading, the plastic strain increment after unloading was significantly lower than the peak strain increment under the same stress level, indicating that the fatigue damage effect is more significant.

Comparing the peak strength of rock under different stress paths in Figure 4, it can be found that under the stress paths with relatively high initial stress amplitude (stress paths 2 and 4), the peak strength of specimens is higher than that of the specimens under the conventional compression test condition (stress paths 1). Under the stress paths with relatively low initial stress amplitude (stress paths 3 and 5), the peak strength of specimens is lower than that under stress paths 1. In addition to that, under the stress path with increased stress lower limit (ISLL) (stress paths 2 and 3), the peak strength of the specimens is lower than that of the specimen under the stress path with constant stress lower limit (CSLL) (stress paths 4 and 5). From the above analysis, it can be seen that under the condition of relatively larger stress amplitude in each stress level of SCLU, the cyclic strengthening effect of specimens will be more prominent and the peak strength will increase accordingly. The strengthening effect and fatigue damage show great differences in the loading process of different stress paths, which will be analyzed in the combined with the variation law of each parameter, later in this article.

3.2. Dynamic Elastic Modulus Analysis. The dynamic modulus of elasticity (E_d) is a parameter commonly used to evaluate the dynamic properties of materials, and the calculation method is shown in Figure 5. E_d reflects the ability of material to resist deformation under dynamic stress. The relationship between E_d and the number of SCLU is shown in Figure 6. Under the four stress paths of SCLU, E_d of the specimen decreases gradually with the upgraded of stress level during the whole process of loading, which is quite different from the existing research results [21]. The main reason is that there are irregular structural planes in

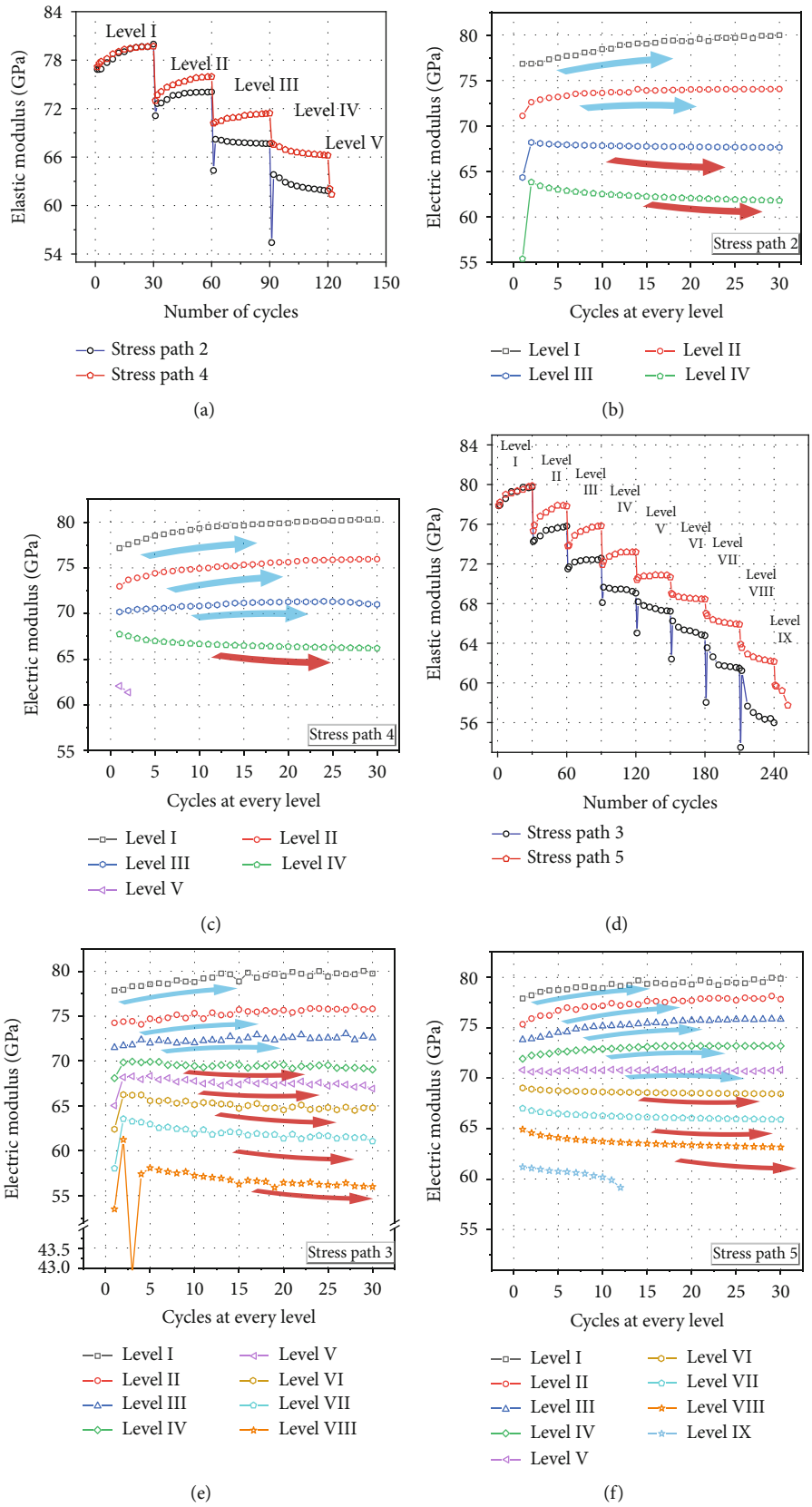

Figure 6: Elastic moduli of specimens evolution process under different stress paths. (a) E_d evolution with number of cycles under stress paths 2 and 4; (b) influences of stress level on E_d under stress path 2; (c) influences of stress level on E_d under stress path 4; (d) E_d evolution with number of cycles under stress paths 3 and 5; (e) influences of stress level on E_d under stress path 3; (f) influences of stress level on E_d under stress path 5.

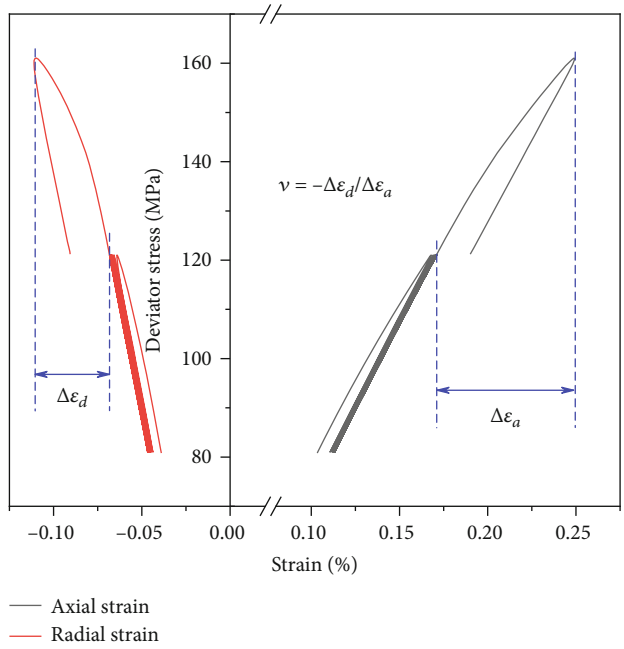

Figure 7: Calculation diagram of dynamic Poisson's ratio.

limestone, with the increase of stress level, the initial cracks in the rock are further compressed and accompanied by the dislocation and friction between adjacent structural planes, the macroscopic deformation of the rock is further increased, leading to the decrease of the elastic modulus.

The variation of E_d under four cyclic loading stress paths was different. As shown in Figures 6(a) and 6(d), with the upgraded of stress level, the decrease trend of E_d under ISLL stress paths (stress path 2 and 3) is higher than that under CSLL stress paths (stress path 4 and 5). In addition, as shown in Figures 6(b) and 6(e), under the stress paths of ISLL, the E_d of the first cycle is smaller than that of other cycles at each stress level. As shown in Figures 6(c) and 6(f), under the stress paths of CSLL, the E_d of the first cycle in each level does not seem to be smaller than that of subsequent cycles. The above results show that under the ISLL stress path, the impact damage of limestone is significant, while under the CSLL stress path, the damage of limestone is mainly progressive.

As shown in Figures 6(b), 6(c), 6(e), and 6(f), under four SCLU stress paths, the E_d of rock increased at the stress level in the early stage of loading, which was caused by the strengthening effect caused by cyclic loading. The E_d of rock decreased at the stress level in the later stage of loading, which was caused by the fatigue damage effect caused by cyclic loading. Stress paths 2 and 3 (Figures 6(b) and 6(e)) show the decreasing trend of E_d due to fatigue damage from level III and level IV, respectively. Compared with CSLL stress paths 4 and 5 (Figures 6(c) and 6(f)), the beginning of decreasing trend of E_d was advanced by 1 and 2 stress levels, respectively. The experimental phenomenon shows that the ISLL will make the limestone enter the fatigue damage stage earlier.

3.3. Dynamic Poisson's Ratio under Step Cyclic Loading Stress Paths. Dynamic Poisson's ratio (μ_d), defined as the ratio of radial strain to axial strain, is used to evaluate the transverse deformation characteristics of materials, and the calculation method is shown in Figure 7. μ_d reflects the information of damage and crack propagation in rock. It can be seen from Figures 8(a) and 8(d) that the variation of μ_d is different from the E_d. Under the condition of SCLU, with the increase of the stress level, the μ_d increases as a whole. The reason is that with the stress level increases, internal structural damage occurs in the specimen, and cracks continue to expand.

The variation of μ_d under four cyclic loading stress paths was different. As shown in Figure 7(a), in the stress path with higher initial stress amplitude (stress path 2 and stress path 4), with the upgraded of stress level, the μ_d showed a trend of decreasing at first and then increasing, basically showing a "U" shape, while in the stress path with lower initial stress amplitude (stress path 3 and stress path 5) as shown in Figure 7(d), the μ_d showed no obvious decreasing trend. Under the stress path with relatively high initial stress amplitude (stress paths 2 and 4), the μ_d decreased in the initial stage of cyclic loading. This is because under the stress paths with relatively higher initial stress amplitude, the cyclic loading has a significant strengthening effect on the rock. Under the stress paths with relatively lower initial stress amplitude (stress paths 3 and 5), due to the relatively small stress amplitude of SCLU, the strengthening effect of cyclic loading on the rock was not obvious. This is consistent with the analysis of rock peak strength under different stress paths in Section 3.1.

It is known from the previous study that the increase of μ_d is due to the propagation of internal cracks [22]. Under SCLU stress conditions, cracks will continue to expand and cause new damage. The main factors affecting the variation law of μ_d vary according to different stress paths. For the stress paths with ISLL (stress paths 2 and 3), the main factor for the increase of μ_d is the impact damage caused by the upgrade of stress level, as shown in Figures 8(b) and 8(e), the maximum value of μ_d appeared in the first cycle of each stress level. While for the stress paths with CSLL (stress paths 4 and 5), the main factor for the increase of μ_d is the fatigue damage caused by cyclic load, as shown in Figures 8(f) and 8(h), the μ_d increased gradually with the accumulation of cycle times. The effect of impact damage on the expansion of microcracks in rock is significantly stronger than that of fatigue damage, which explains why the μ_d increases faster under the ISLL stress path than under the CSLL stress path.

3.4. Peak Strain under Step Cyclic Loading Stress Paths. It can be seen from Figure 4 that the hysteresis curve will change with the different stress paths. With the accumulation of cycles, the hysteresis curve formed by each cycle has a tendency to move gradually towards the direction in which the absolute value of its corresponding strain increases. In other words, the specimen will undergo irreversible deformation under stress paths of SCLU. The calculation method of irreversible deformation is shown in Figure 9. The peak strain

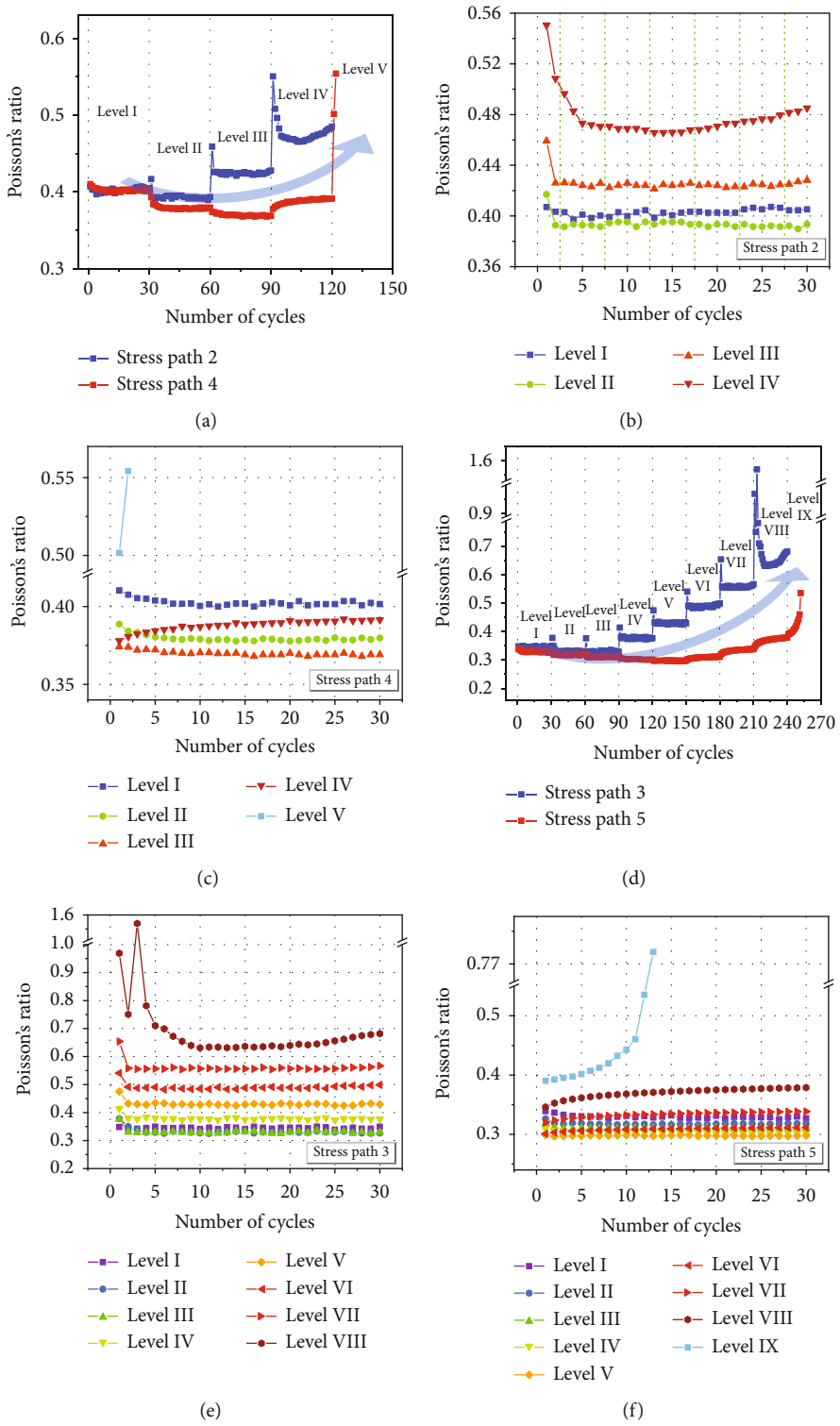

Figure 8: Poisson's ratio of specimen evolution process under different stress paths. (a) μ_d evolution with number of cycles under stress paths 2 and 4; (b) influences of stress level on μ_d under stress path 2; (c) influences of stress level on μ_d under stress path 4; (d) μ_d evolution with number of cycles under stress paths 3 and 5; (e) influences of stress level on μ_d under stress path 3; (f) influences of stress level on μ_d under stress path 5.

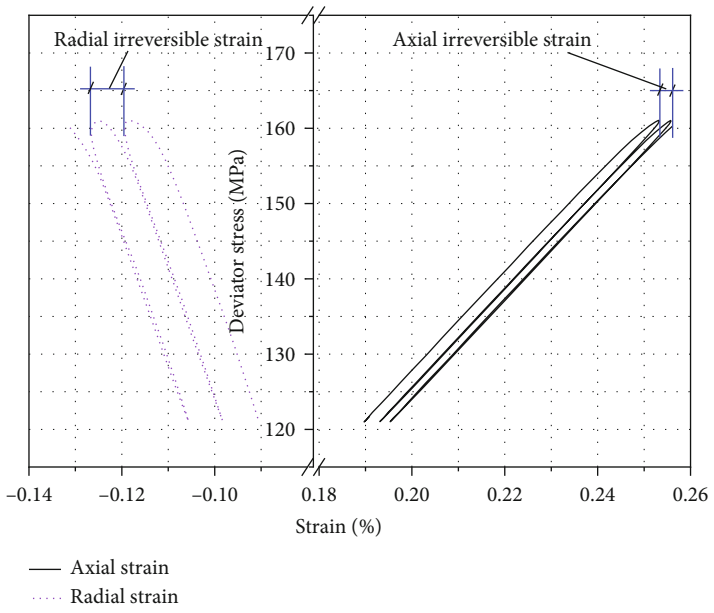

Figure 9: Calculation diagram of irreversible strain.

increment was used to analyze the plastic strain increment of the rock plastic deformation. The reason why the strain increment after unloading is not used is that the lower stress limit variations under different stress paths are different, so the strain increment after unloading is not comparable.

Figures 10(a) and 10(b) show the comparison of peak strain and cycle times of rock under four step cyclic loading stress paths. Figures 10(c)–10(f) show the relationship between the increment of peak strain and cycle times under different stress paths. Under the four stress paths of SCLU, the peak strain increases gradually on the whole. It indicates that with the upgraded of stress level, the rock was compressed gradually in axial direction and expanded gradually in radial direction. As shown in Figures 10(a) and 10(b), the peak strain growth rates under the ISLL stress paths 4 and 5 were higher than that under the CSLL stress paths 2 and 3, respectively. According to Figures 10(c) and 10(d), under the ISLL stress paths, the peak strain increment mainly existed in the first cycle of each stress level, and the peak strain increment caused by the increase of stress level increases linearly. As shown in Figures 10(e) and 10(f), under the CSLL stress path, the peak strain increment existed in the entire cycling process of each stress level, in which the peak strain increment caused by the upgraded of stress level was basically consistent, while the peak strain increment caused by cyclic loading increased gradually with the upgraded of stress level.

As shown in Figure 10(a), under stress path 2, the cumulative irreversible axial and radial strains increase significantly with the accumulation of cycle times at the last stress level (level IV) before failure, and the cumulative irreversible radial strain increment is significantly higher than the cumulative irreversible axial strain. This indicates that microcracks begin to develop effectively. However, in the level IV of stress path 4, the cumulative irreversible axial and radial strain generated by SCLU is small, so that the cumulative irreversible axial and radial strain is significantly lower than that of stress path 2. This phenomenon indicates that, compared with the loading condition with CSLL, the stress threshold corresponding to the effective development of microcracks in rock is lower under the loading condition with ISLL, and the rock enters the irreversible strain accumulation stage caused by SCLU earlier. As shown in Figure 10(b), for stress paths 3 and 5, the difference in irreversible deformation between them caused by the different changes in the lower stress limits was similar to that of stress paths 2 and 4. However, the cumulative irreversible axial and radial strain of stress paths 3 and 5 before failure were higher than that of stress paths 2 and 4. The reason for this phenomenon is that the increment of upper stress limit at adjacent stress levels of stress paths 3 and 5 is less than that of stress paths 2 and 4. The results show that the smaller the increment of upper stress limit at adjacent stress levels, the more significant the plastic deformation of the rock under the stress path.

The above phenomena show that under the ISLL stress path, the irreversible deformation caused by cyclic loading before failure is small because the stress amplitude remains constant and does not grow. It produces less axial irreversible deformation than that under the CSLL stress path. However, it does not have a significant effect on the development of radial peak strain, which also explains why the μ_d increases faster under the ISLL stress path than under the CSLL stress path. In addition, it can be found that under the ISLL stress path, the irreversible strain of the specimen accumulates significantly at the last stress level, and the specimen fails suddenly when the stress level entered the next. However, under the CSLL stress path, the peak strain of the specimen increased gradually during the failure process, and there was a buffer process. Comparing Figures 10(a) and

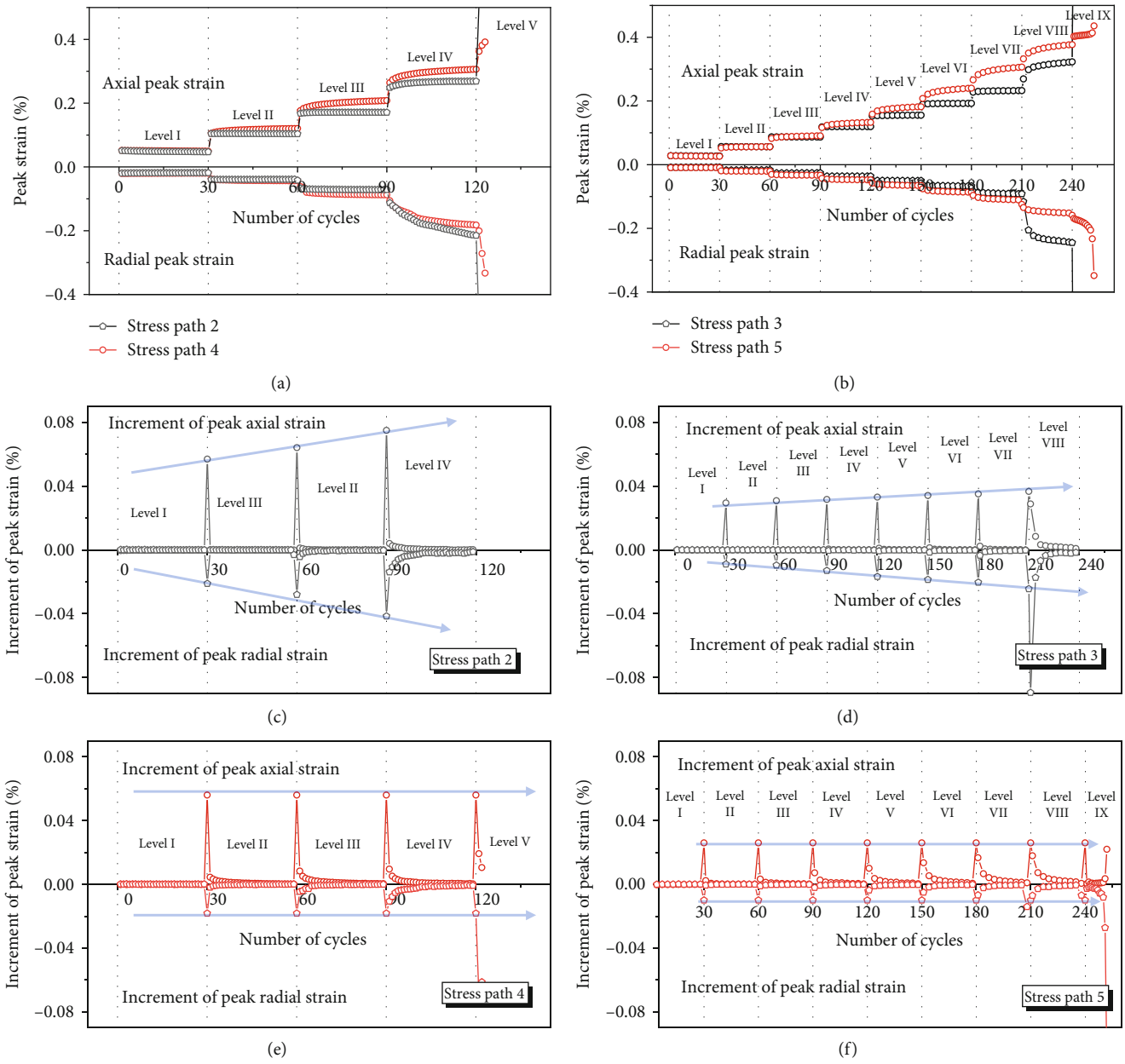

Figure 10: Peak strain of specimen evolution process under different stress paths. (a) Peak strain evolution with number of cycles under stress paths 2 and 4; (b) peak strain evolution with number of cycles under stress paths 3 and 5; (c) increment of peak strain under stress paths 2; (d) increment of peak strain under stress paths 3; (e) increment of peak strain under stress paths 4; (f) increment of peak strain under stress paths 5.

10(b), it can be found that the deformation before failure of the specimen under stress paths 3 and 5 with small initial stress amplitude was significantly higher than that under stress paths 2 and 4 with large initial stress amplitude. Moreover, the buffering process of rock failure was more obvious under the CSLL stress path with low initial stress amplitude.

4. Energy Evolution Laws under Different Stress Paths

4.1. Definition of Energy Parameters in SCLU Process. In the process of SCLU test, the upper and lower limits of stress are usually set, and the SCLU is carried out by stress control method. The research results of the existing research results [23, 24] show that in the process of SCLU, the hysteretic loop curve is usually not closed, and the stress-strain hysteretic loop curve in the typical process of SCLU is shown in Figure 11. The curve in loading stage is usually higher than that in unloading stage, and there is residual deformation. From the perspective of energy, under the action of SCLU in stages, part of the total energy input from the outside is stored in the material in the form of elastic strain energy, which can be released during unloading and is reversible. The other part of the energy is dissipated by the plastic deformation of the specimen, the expansion of the crack, and the transformation into the form of sound energy, heat

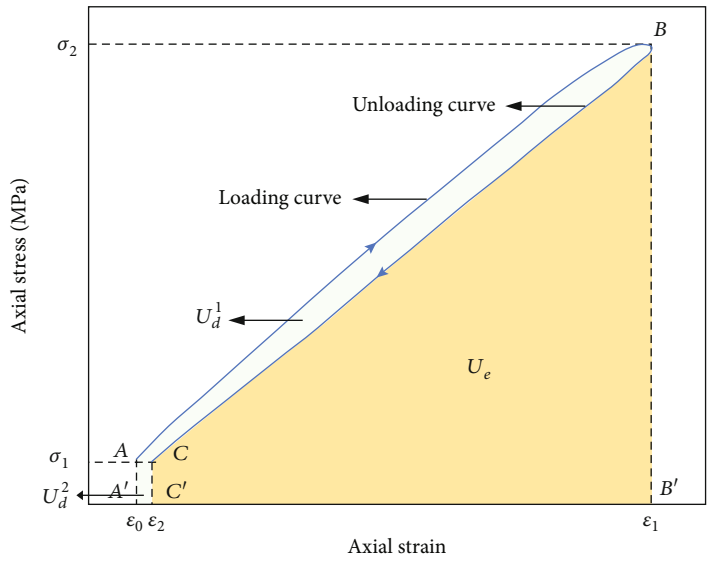

Figure 11: Hysteresis loop of rock under cyclical loading and unloading conditions.

energy, and radiation energy, which is called dissipated energy. The dissipated energy will not be released from the rock specimen in the unloading stage and is irreversible.

Taking the cyclic stress-strain curve shown in Figure 11 as an example, the area enclosed by ABB′A′ included in the loading curve is defined as the absorbed energy (U) during the loading process, the area enclosed by CBB′C′ included in the unloading curve is defined as the elastic strain energy (U_e) during the unloading process, and the area of the difference between the areas enclosed by the loading and unloading curves A′ABCC′ is defined as the dissipated energy (U_d). According to the concept of definite integral, the area of tiny trapezoid bars is used to sum:

$$U = \sum_{i=1}^{n} \frac{1}{2} \left[(\sigma_1 - \sigma_3)_i + (\sigma_1 - \sigma_3)_{i+1} \right] \left[(\varepsilon_a)_{i+1} - (\varepsilon_a)_i \right], \quad (1)$$

$$U_e = \sum_{j=1}^{n} \frac{1}{2} \left[(\sigma_1 - \sigma_3)_j + (\sigma_1 - \sigma_3)_{j+1} \right] \left[(\varepsilon_a)_{j+1} - (\varepsilon_a)_j \right], \quad (2)$$

$$U_d = |U| - |U_e| = U_d^1 + U_d^2. \quad (3)$$

4.2. Energy Evolution Process and Characteristics under SCLU Stress Paths. In the process of SCLU, along with the transformation of energy input, release, and dissipation; the rock material undergoes the process of germination, expansion, penetration, and instability failure of primary fissures. There is energy state corresponding to the stress state. The energy state at this time is a function of stress, strain, and time and is related to the stress path of the rock specimen and the current stress-strain state [25]. Therefore, energy evolution reflects the essential properties of the closure of the original microdefects in the rock and the generation, expansion, and penetration of new microcracks.

Figure 12 shows the evolution of the U, U_e, and U_d of the rock specimens during each SCLU according to the energy calculation results under different stress paths. It can be seen from Figure 12 that under different stress paths, with the upgraded of stress level, the energy of each part of showed an increasing trend. This shows that although the stress paths are different, the energy required is increased with the generation, expansion, and penetration of the rock cracks.

Under the ISLL stress paths (stress path 2 and 3), the U and U_e of specimens presented a linear increase trend with the upgraded of stress level. Under the CSLL stress paths (stress path 4 and 5), the U and U_e of specimens presented exponential increase trend with the upgraded of stress level, and the rates of energy input (U) and output (U_e and U_d) were higher than those under the ISLL stress paths. This is because under the CSLL stress paths, the stress amplitude gradually increases, and the rock can be completely unloaded and reloaded. Therefore, the friction between the internal structures of the rock is more sufficient, and the energy consumption is greater.

As shown in Figures 12(a1) and 12(a3), under the ISLL stress paths, when the stress level entered the next, there was impact energy input, which was greater along with the upgraded of the stress level. Similarly, as shown in Figures 12(c1) and 12(c3), the U_d under this stress paths also showed this regularity, and the U_d was mainly concentrated in the first cyclic loading at each stress level, but it was very low in the later cyclic loading process. This indicates that under ISLL stress path, the rock is mainly affected by the impact damage caused by the increase of stress level. As shown in Figures 12(a2) and 12(a4), under the CSLL stress paths, with the upgraded of stress level, the U_d increased gradually in a step-like variation trend on the whole. Under the same stress level, with the increasing of the number of cycles, there was no obvious attenuation in the evolution process of U_d. This indicates that the stress paths with CSLL weaken the impact damage and intensify the fatigue damage of rock.

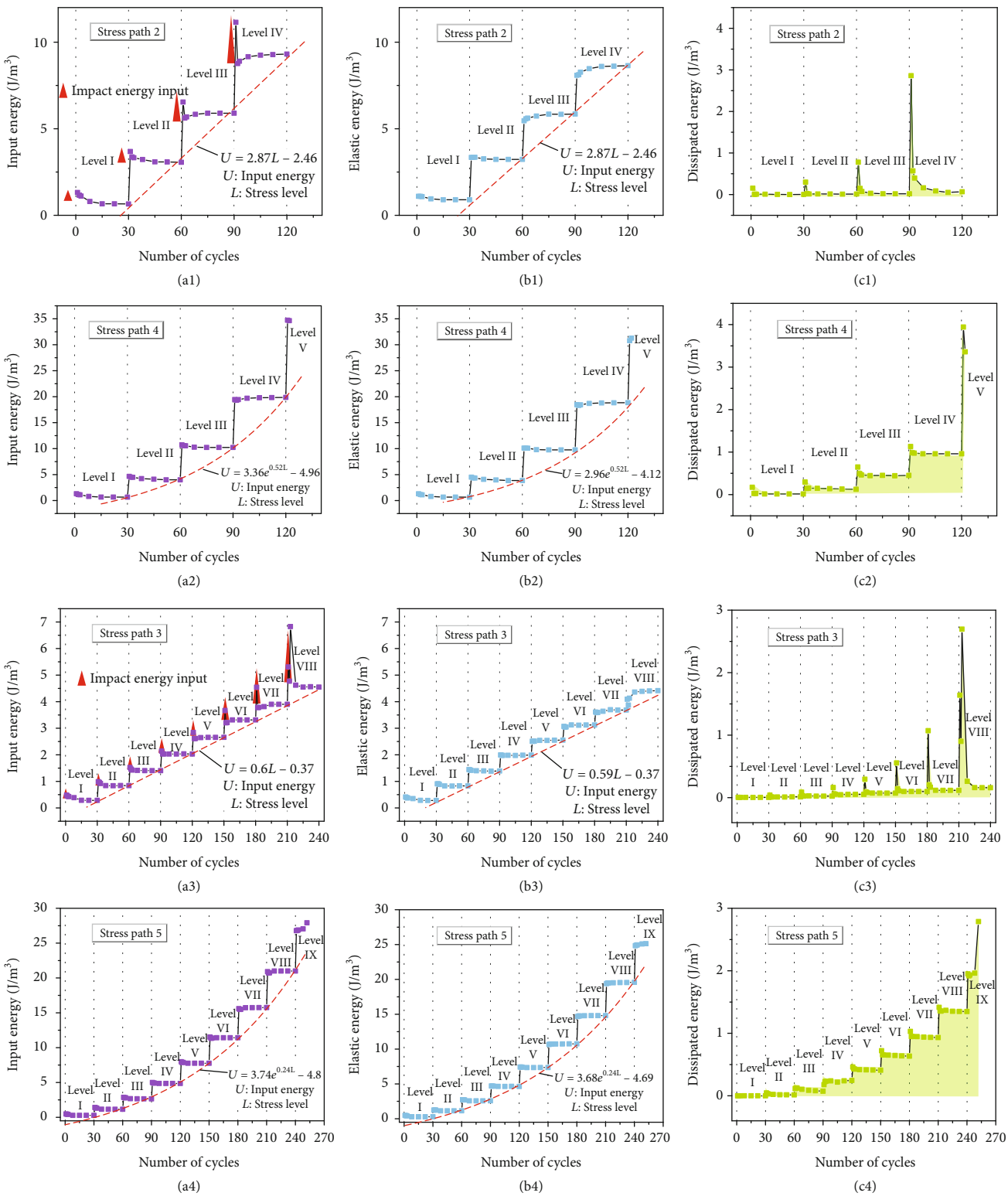

FIGURE 12: Energy evolution diagram in step cyclic loading stress paths. (a1)–(a4) The evolution of U with the accumulation of cycle times under stress paths 2-5; (b1)–(b4) the evolution of U_e with the accumulation of cycle times under stress paths 2-5; (c1)–(c4) the evolution of U_d with the accumulation of cycle times under stress paths 2-5.

The U and U_e with higher initial stress amplitude (stress path 2 and stress path 4) were greater than those with lower higher initial stress amplitude (stress path 3 and stress path 5). It shows that the ISLL stress path with relatively higher increment at adjacent stress levels is more likely to cause impact damage to the rock, and the CSLL stress path with relatively lower increment at adjacent stress levels is more likely to cause fatigue damage to the rock.

The slippage deformation between the internal structural planes of rock is mainly related to the stress amplitude, and the larger the stress amplitude, the more significant the slippage process is. Under the CSLL stress path, the stress amplitude of rock gradually increases with the upgraded of stress level, and the rock deformation and external input energy also increase, which makes the frictional sliding process of structural plane more significant. After unloading and reloading, the improvement of the contact state between the structural planes increases the friction force and contributes to the increase of the bearing capacity of the rock. However, under the ISLL stress path, due to the constant stress amplitude, the rock deformation and external input energy are relatively low, which makes the strengthening effect of the rock is relatively weak.

5. Conclusions

(1) Cracked rocks have obvious strengthening effect under cyclic loading. In the process of loading, the irregular structural planes in rock will be subjected to local contact stress much higher than the nominal stress, resulting in local failure. The detritus formed may fall off during unloading and fill into nearby voids, improving the friction properties and increasing the bearing capacity of the rock

(2) Cyclic loading leads to fatigue damage of rock, and the upgraded of stress level leads to impact damage of rock. The latter has a stronger effect on the expansion of microscopic cracks in rock than the former. Under the stress path of ISLL, the rock will suffer linearly increasing impact damage with the increase of stress level, while under the stress path of CSLL, the rock mainly suffers progressive fatigue damage

(3) During the initial loading period, the stress strengthening effect of rock is more obvious, while the fatigue damage effect is more prominent in the later loading period. Under the stress path of CSLL, the strengthening effect of rock is more prominent and its strength enhanced, while under the stress path of ISLL, the fatigue damage of rock is more prominent and its strength decreased

(4) The stress path with smaller initial stress amplitude experienced more fatigue loading cycles, which intensifies the fatigue damage of limestone. Therefore, the plastic deformation and energy dissipation of rock material are greater, the rock is more prone to progressive damage and the buffering effect is more obvious during the failure

Nomenclature

SCLU: Step cyclic loading and unloading
U: Absorbed energy during the loading process
CSLL: Stress path of constant stress lower limit
U_e: Elastic strain energy (U_e) during the unloading process
ISLL: Stress path of increasing the stress lower limit
U_d: Dissipated energy
E_d: Dynamic modulus of elasticity
μ_d: Dynamic Poisson's ratio

Data Availability

All data, models, and code generated or used during the study appear in the submitted article.

Conflicts of Interest

The authors declare that they have no conflict of interest.

Acknowledgments

This research was supported by the National Key R&D Program of China (Grant no. 2018YFC1505001), the Second Tibetan Plateau Scientific Expedition and Research (STEP) program (Grant no. 2019QZKK0905), the West Light Foundation of Chinese Academy of Sciences (Granted to Dr. Minghao Liu), the Program of the State Key Laboratory of Frozen Soil Engineering (Grant no. SKLFSE-ZT-202110), and the Science Technology Research and Development Plan of Qinghai-Tibet Railway Group Corporation (QZ2021-G02).

References

[1] J. Q. Xiao, D. X. Ding, F. L. Jiang, and G. Xu, "Fatigue damage variable and evolution of rock subjected to cyclic loading," *International Journal of Rock Mechanics and Mining Sciences*, vol. 47, no. 3, pp. 461–468, 2010.

[2] A. Taheri, A. Royle, Z. Yang, and Y. Zhao, "Study on variations of peak strength of a sandstone during cyclic loading," *Geomechanics and Geophysics for Geo-energy and Geo-sources*, vol. 2, no. 1, pp. 1–10, 2016.

[3] G. Lee, A. Kumar, E. Berkson, N. Verma, B. Bach Jr., and N. Hallab, "A biomechanical analysis of bonepatellar tendon-bone grafts after repeat freeze-thaw cycles in a cyclic loading model," *Journal of Knee Surgery*, vol. 22, no. 2, pp. 111–113, 2009.

[4] Y. J. Shen, G. S. Yang, M. Wang, H. L. Jia, H. M. Zhang, and X. C. Gao, "Experiments on the damage characteristics and fracture process of single-joint quasi-sandstone under the cyclic freezing-thawing and cyclic loading," *Chinese Journal of Rock Mechanics and Engineering*, vol. 37, 2018.

[5] J. Hu, P. Zeng, D. Yang et al., "Experimental investigation on uniaxial compression mechanical behavior and damage evolution of pre-damaged granite after cyclic loading," *Energies*, vol. 14, no. 19, p. 6179, 2021.

[6] Y. J. Shen, H. Yang, L. Jin, H. Zhang, G. Yang, and J. Zhang, "Fatigue deformation and energy change of single-joint

sandstone after freeze-thaw cycles and cyclic loadings," *Frontiers in Earth Science*, vol. 7, 2019.

[7] N. Erarslan, "Microstructural investigation of subcritical crack propagation and fracture process zone (FPZ) by the reduction of rock fracture toughness under cyclic loading," *Engineering Geology*, vol. 208, pp. 181–190, 2016.

[8] X. Ge, Y. Jiang, Y. Lu, and J. Ren, "Testing study on fatigue deformation law of rock under cyclic loading," *Chinese Journal of Rock Mechanics and Engineering*, vol. 22, no. 10, pp. 1581–1585, 2003.

[9] M. Ghamgosar and N. Erarslan, "Experimental and numerical studies on development of fracture process zone (FPZ) in rocks under cyclic and static loadings," *Rock Mechanics and Rock Engineering*, vol. 49, no. 3, pp. 893–908, 2016.

[10] M. Ghamgosar, N. Erarslan, and D. J. Williams, "Experimental investigation of fracture process zone in rocks damaged under cyclic loadings," *Experimental Mechanics*, vol. 57, no. 1, pp. 97–113, 2017.

[11] H.-P. Xie, R.-D. Peng, Y. Ju, and H.-W. Zhou, "On energy analysis of rock failure," *Chinese Journal of Rock Mechanics and Engineering*, vol. 24, no. 15, pp. 2603–2607, 2005.

[12] R. D. Peng, H. P. Xie, and Y. Ju, "Analysis of energy dissipation and damage evolution of sandstone during tensile process," *Chinese Journal of Rock Mechanics and Engineering*, vol. 26, no. 12, pp. 2526–2531, 2007.

[13] X. U. Jiang, L. Bobo, and Z. H. Ting, "Experimental study of deformation and energy evolution law of coal under cyclic loading," *Chinese Journal of Rock Mechanics and Engineering*, vol. 33, no. 2, pp. 3563–3572, 2014.

[14] H. Yasuhara, C. Marone, and D. Elsworth, "Fault zone restrengthening and frictional healing: the role of pressure solution," *Journal of Geophysical Research*, vol. 110, no. B6, 2005.

[15] R. Shen, T. Chen, T. Li et al., "Study on the effect of the lower limit of cyclic stress on the mechanical properties and acoustic emission of sandstone under cyclic loading and unloading," *Theoretical and Applied Fracture Mechanics*, vol. 108, 2020.

[16] J. P. Zuo, L. F. Liu, H. W. Zhou, and Y. M. Huang, "Deformation failure mechanism and analysis of rock under different mining condition," *Journal of China Coal Society*, vol. 38, no. 8, pp. 1319–1324, 2013.

[17] Y. G. Li, "Postseismic fault healing on the rupture zone of the 1999 M 7.1 Hector mine, California, earthquake," *Journal of American History*, vol. 101, no. 1, pp. 340-341, 1999.

[18] K. Tadokoro and M. Ando, "Evidence for rapid fault healing derived from temporal changes in S wave splitting," *Geophysical Research Letters*, vol. 29, no. 4, 2002.

[19] C. Marone, "Laboratory-derived friction laws and their application to seismic faulting," *Annual Review of Earth & Planetary Sciences*, vol. 26, no. 1, pp. 643–696, 1998.

[20] B. Bos and C. J. Spiers, "Fluid-assisted healing processes in gouge-bearing faults: insights from experiments on a rock analogue system," *Pure & Applied Geophysics*, vol. 159, no. 11-12, pp. 2537–2566, 2002.

[21] D. Y. Jiang, J. Y. Fan, J. Chen, L. Li, and Y. Cui, "A mechanism of fatigue in salt under discontinuous cycle loading," *International Journal of Rock Mechanics and Mining Sciences*, vol. 86, pp. 255–260, 2016.

[22] Q. L. Li, Z. J. Jia, and H. L. Fu, "Experimental study on dynamic characteristics of sandstone under cyclic loading and different confining pressures," *Journal of Railway Science and Engineering*, vol. 16, no. 10, pp. 2459–2466, 2019.

[23] Z. Z. Zhang and F. Gao, "Experimental investigation on the energy evolution of dry and water-saturated red sandstones," *International Journal of Mining Science and Technology*, vol. 25, no. 3, pp. 383–388, 2015.

[24] H. F. Deng, Y. Hu, J. L. Li, Z. Wang, X. J. Zhang, and A. L. Hu, "The evolution of sandstone energy dissipation under SCLU," *Chinese Journal of Rock Mechanics and Engineering*, vol. 35, pp. 2869–2875, 2016.

[25] X. S. Liu, J. G. Ning, Y. L. Tan, and Q. H. Gu, "Damage constitutive model based on energy dissipation for intact rock subjected to cyclic loading," *International Journal of Rock Mechanics and Mining Sciences*, vol. 85, no. 1, pp. 27–32, 2016.